International Review of Electrical Engineering (I.R.E.E.), Vol. 5, N. 3
May-June 2010

An Arcless Current Interruption Technique via Application of Resistive and Liquid Metal Contacts

P. Pourmohamadiyan, K. Niayesh, H. Mohseni

Abstract – *In this paper, theoretical and experimental studies of an arcless current interruption technique are presented. The introduced method eliminates the switching arc and its consequences through application of liquid metal and resistive contacts. First, the solid-liquid contact system is analyzed and the basic phenomena related to arcless switching are elaborated. Then the design requirements are recognized and are converted to a set of mathematical expressions and accordingly the design parameters are determined. The major electromagnetic quantities like current density distribution, magnetic flux density and the force are obtained by a FEM solver and the calculated force is used in numerical calculations of motion simulation. Finally, the designed structure is evaluated through a set of experiments which test the performance of the switch especially in the arcless current interruption.*

Keywords: *Arcless Current Interruption, Liquid Metal Contact, Inherently Controlled Switch*

Nomenclature

u_{LM}	Voltage drop on the LM tail
I_{LM}	LM tail current
R_{LM}	LM tail equivalent resistance
R_{Δ}	Incremental resistance element from the resistance profile which is bridged over by the LM tail
I_{tot}	Total current of resistance profile
$u_{contacts}$	Voltage of contacts after separation
L_{sc}	Equivalent inductance of the test circuit
R_{sc}	Equivalent resistance of the circuit
R_{tot}	Total resistance of the moving contact when the resistance profile is completely pulled out from the LM
u_{Source}	Source voltage
$i(t)$	Switch current
$R_{LM}(t)$	Variable resistance of LM bridge during commutation
$I_{LM}(t)$	Variable current of the LM bridge
T_0	The duration of current interruption
T_f	Final temperature of the LM tail
T_i	Initial temperature of the LM tail
$m_{LM\ tail}$	Mass of the LM tail
C_{LM}	LM specific heat
$Q_{Resistive\ heat\ loss}$	Heat loss dissipated by the resistance profile
$R_{Resistance\ Profile}(t)$	time / position depended part of the resistance profile lying above LM level
m_{LM}	LM mass
m_{IF}	Insulating Fluid mass
C_{IF}	Insulating Fluid (air) specific heat
b_1 and b_2	Radiuses of the two axial coils
F_{12}	Force exerted on coil number 2 (the moving coil) by coil number 1 (fixed coil)
I_1 and I_2	Currents flowing through coils (in our case $I_1 = I_2$)
N_1 and N_2	Number of turns for fixed and moving coil respectively
d	Distances between coils

I. Introduction

Switching arc has been known as a limiting factor in the circuit breaker design and fabrication [1]. Many efforts have been made to develop arc quenching techniques. Some of these techniques introduce relatively large size interruption chamber or operation mechanism to the circuit breakers. Moreover due to the nature of the arc, post-arc phenomena impose some special limitation on the insulation material and the structure of the interruption chamber. To reduce the arc consequences

Manuscript received and revised May 2010, accepted June 2010

and support circuit breakers, the current limiting devices have been considered and developed as a supplementary element in the switching technology. Current limiters are also beneficial to reduce the amount of short circuit current flowing through distribution network equipment. Accordingly, various types of passive and active limiters [2] have been introduced. Active limiters exhibit low impedance during nominal services and in contrast a high impedance during short circuit condition. They may perform current limitation and its successive breaking of the current or may only limit the flowing current and leave the breaking action for other switching components. Current limiters can be externally controlled or inherently operated among built in trigger. They may be automatically reseted or replaced after short circuit manually. Resonance links [2], superconducting fault current limiters [3], [4], positive temperature coefficient (PTC) resistances [5], [6] and Liquid Metal (LM) fault current limiters [7] are the well known automatically resettable inherently triggered current limiting techniques. The LM current limiter was first developed based on the application of the Pinch effect for current interruption. The method takes the advantage of high current in the constriction region and narrows the current carrying cross section till complete rupture of the LM path and arc initiation. Accordingly, the arcing voltage acts as a current limiting factor. There is also another type of LM current limiter which limits the current without arc via motion of LM in the resistive capillary walls [8]. But the mentioned motion of the LM bridge in the resistive capillary has some difficulties. Essentially once the LM bridge starts to move, it deforms due to the friction force between LM and the surrounding walls. This force affects the regions in the vicinity of LM boundaries with surrounding walls, but due to the low LM intermolecular force, non-boundary regions are affected less and tend to move faster. When the current is high enough, the unwanted Pinch effect would cause another LM bridge deformation. These deformations lead to non-homogenous current density and force distribution in the LM bridge. Although the LM deformations could not impair the device operation but they may cause considerable tolerance in the device performance during operations. The present paper introduces a new arcless switch via application of the LM and resistive contacts. A current limiting method similar to [8] is used to reduce the current before arcless switching but to overcome the mentioned difficulties, a new structure is proposed for the relative motion of the LM and the resistance profile. This structure is composed of a moving resistive profile which is pulled out from a LM vessel during current interruption. This can be realized through inherent Lorentz forces or may be done by an externally triggered auxiliary system. At first, the conditions required for arcless current commutation are described. These conditions are converted to a constrained optimization problem which its solution reveals the resistance profile. Meanwhile, this problem needs some physical parameters which have to be determined through simple experiments. Based on the switch abnormal current, the moving contact speed and the critical parameters of resistive material and LM, the resistance profile geometry is specified. Since the resistance profile is immersed in the LM during normal service and has to be pulled out during short circuit condition, the geometry is selected considering immersed object dynamics. This matter is not discussed within the paper. The motion path is determined based on the final geometry of the moving object. This is followed by driving mechanism description. Magnetic repulsion coils and a permanent magnet spring (PMS) structure [9] are used to ascertain high speed interruption. Finally the experimental results are presented and discussed. The Proposed method takes the advantage of arcless controlled switching with relatively small interruption chamber which has simple structure. Moreover, as a liquid metal intermediate medium is used between the contacts, surface degradation of contacts is considerably reduced while the contact resistance is decreased.

II. Working Principle

A special resistance profile is implemented on the moving contact of the switch. This resistance profile converts the interruption energy into heat and eliminates the arc by imposing a resistive voltage drop instead of arcing voltage. Figure 1 shows a scheme of the switch operation. As it can be seen the resistance profile is immersed in a LM contained vessel. During nominal current, the resistance profile is fully immersed in the LM and the conductive contact (copper part of the moving contact which is placed above the resistance profile) is in contact with LM bulk. Therefore as the liquid metal wets the surface of the conductive part, no transition resistance occurs and the equivalent contact resistance is less than that of conventional low voltage air insulated switches which its contact resistance is mainly depended on contact force.

To have a uniform symmetrical current distribution in the LM vessel, the fixed coil is connected to the bottom center of the vessel. It is also possible to design a more functional structure in which the nominal current can also flow through another separate path which doesn't heat up the LM bulk in normal condition. This optional path may consist of the conductive contact shown in Fig. 1 and a flexible circular plate touching the metallic vessel edge. But for the present study the simple structure shown in figure 1 is applied. Upon external trigger or inherently during predetermined short circuit condition, this resistance profile is pulled out by a high speed electromagnetic repulsion drive mechanism. The driving electromagnetic force relates quadratically with the flowing current. It is generated via interaction of two magnetic fields originated from the coils located on the fixed and moving contacts. To achieve inherent control on the current, the coils are placed in series with the

switch and the geometry are designed in such a way that flowing of the predetermined threshold current through the coils provide an electromagnetic force enough to overcome the opponent forces (e.g. gravitation force, friction, etc.,). Once the electromagnetic force overcomes the opponent forces, the resistance profile moves upward from the LM bulk. This in turn causes actuation of PMS which retains the resistance profile above the LM level.

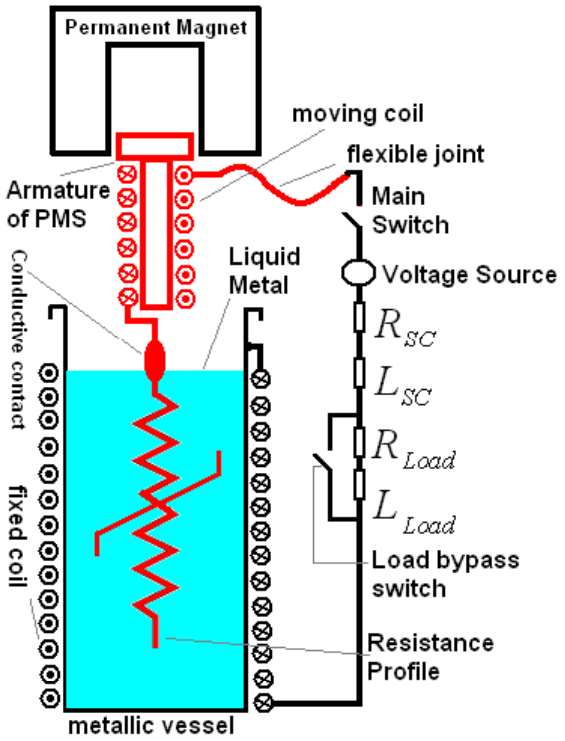

Fig. 1. Scheme of the switch operation: Once the switch current exceeds the threshold amount, the electromagnetic force between the moving and fixed coils moves the moving contact upward

III. Liquid Metal Intermediate Contact Medium

A real solid surface can not be ideally burnished because of asperities appearing during machining and subsequent use. The solid surface experiences the effects of various factors that can be classified into manufacturing, operational, and structural. These errors in form, waviness, roughness and subroughness [10] become much more important especially when two solid contacts have to slide on each other while carrying electrical current. In contacts between liquid and solid metals, the deformation of the solid member is negligible. Here the load bearing and the apparent area are equal. Therefore, the utilization of a liquid metal as an intermediate medium separating solid contact members significantly increases the contact area encompassing almost the whole apparent area of the solid electrode surface. If a liquid metal wets the virgin surface of the solid electrode, no transition resistance occurs provided that the metals do not produce chemical compounds. When a liquid metal moistens the oxidized surface of the solid electrode surface, the contact resistance is controlled by the resistance of the oxide film, which is in the order of $10^{9}-10^{7}\ \Omega m^{2}$ for thick metal oxide films [10]. In the proposed switch, liquid metal intermediate contact medium does not only reduce the contact resistance and friction coefficient but also it rather maintains them in a firm contact during motion of the resistance profile. This is a vital feature for the arcless motion of the resistance profile. In [11], it was concluded that interruption of metal bridges between contacts at the highest temperature point causes a metal transfer from the electrode closer to the maximum temperature of the bridge toward the other one. In such cases the remaining stubs, usually are reintegrated into the electrodes by surface tension. This is usually observed in "arcless" switching contacts. Therefore, such "bridge transfer" or "fine transfer" is considered as a major reason of "arcless" switching instead of the "arc transfer" in currents strong enough to cause obvious arcing. The LM intermediate contact medium considerably facilitates the prescribed material transfer during switching and therefore the arcless switching would be convenient. To have a desirable form of material transfer, LM material should have low surface tension with the resistance profile. Therefore, metallurgical and chemical countermeasures have to be considered in material selection for each component. In our study the intermediate liquid metal is Mercury of 99% purity. Mercury has a relatively high boiling point of about 357 °C and high density which results in less evaporation and less drop scattering. These properties make this liquid metal a proper choice for intermediate contact medium though its toxicity and environmental effects should be considered for further development. Mercury also does not wet the surface of the material selected for resistance profile. A composition of 80% Nickel and 20% Chrome is used as resistive material. The selected resistive material has resistive temperature coefficient of about $5\times10^{-5}\ \mathrm{K/°C}$ from 20 to 1000 °C and thermal conductivity of about 15 W/mK at 120 °C. Its coefficient of linear expansion which has great importance in resistance profile design is $12.5\times10^{6}/\mathrm{K}$ from 20 to 1000 °C. Its melting temperature is 1400 °C which is much larger than maximum working temperature of the contacts.

IV. Resistance Profile of the Contacts

The resistance profile should convert the interruption energy into heat. From the circuit point of view, the resulted resistive voltage drop should be large enough to limit the separating contacts voltage to an amount less than the minimum voltage needed for arc initiation. Meanwhile, the resistance profile should reduce the

current to less than minimum value needed for arc initiation just in the moment of separation of the resistance profile and the liquid metal. The profiles should be determined considering the following major criteria:

1. During the current interruption, thermal overstressing must be prevented in the tail of LM formed on the resistance profile. In other words, the voltage drop on these parts of circuit must be limited to a specified u_{max} (like the boiling voltage for conventional separating contacts [12]).
2. During the current interruption, the difference between the applied voltages on the separating contacts should not exceed a minimum level u_{min}^{arc} (dependent on the contacts material [13]). Short length/duration arcs should also be prevented during separation of the resistance profile from LM bulk.
3. The voltage appears across insulation parts should not exceed their respective breakdown voltages.
4. During current interruption, thermal overstressing must be prevented in the resistance profile though the boiling point of the LM is much lower than the resistor material melting point.

IV.1. Thermal Overstressing

During motion of the resistance profile, very high current densities may be reached especially in the LM tail formed on the resistance profile. Figure 2 illustrates the equivalent circuit of the contact system during resistance profile motion. To prevent thermal over stressing in the LM tail, its resistive heat dissipated energy has to be kept low. The thermal overstressing of the last LM connection is similar to the instabilities of endmost connecting bridge during the contact separation in conventional switches and therefore the same formulation can be applied. So it would be possible to define a maximum voltage u_{max} (like boiling voltage for conventional separating contacts [12]), above which the last LM connection between the moving resistance profile and the LM bulk become unstable. Therefore the constraint of thermal overstressing can be expressed as:

$$u_{LM} \leq u_{max} \tag{1}$$

where u_{LM} is the voltage drop on the LM tail that is equal to $I_{LM} \times R_{LM}$. Here I_{LM} is current flowing through the LM tail between the LM bulk and the moving resistance profile and R_{LM} is its equivalent resistance.

To have an acceptable estimation of the LM tail shape on the resistance profile, a set of experiments has been done with similar geometry, materials and motion speed. The main goal of these experiments is to estimate the shape and size of the liquid metal tail on the resistance profile and moving contact.

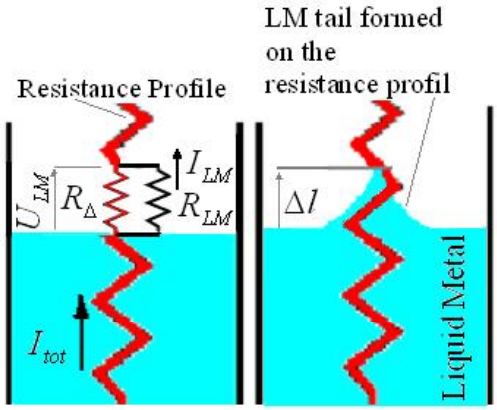

Fig. 2. Equivalent circuit of the contact system during upward motion of the resistance profile in the LM

Meanwhile, the contact resistance and circuit parameters have also been measured.

To determine the circuit parameters, in addition to some basic experiments, a FEM solver has also been used to model the geometry. The current density distribution, heat dissipation and equivalent LM resistance in the proposed geometry are estimated among simulation and are checked with the design criteria in various steps. As the resistance profile is being pulled out from the LM bulk, the circuit resistance is increased. Meanwhile, the current density distribution inside the LM bulk varies due to the smaller length of the resistance profile under the LM level. Therefore the distribution of current between the main path of the resistance profile and the LM tail varies too. Simultaneously the flowing current is decreased. The length of LM tail becomes important especially when we consider the possibility of sudden evaporation of the LM tail on the resistance profile due to thermal overstressing. This would lead to a sudden change in circuit resistance which in turn may lead to arc initiation between LM bulk and the portion of the resistance profile previously bypassed by LM tail. A similar step change may be occurred in the circuit resistance due to the sudden separation of the LM tail during motion. To minimize the effect of this unwanted step change in current limiting resistance, the LM tail length should be shortened. This can be achieved through selection of contacts geometry and materials. Considering constraint expressed in (1), the equivalent circuit of Fig. 2 is analyzed to calculate the maximum allowable resistance profile gradient for given values of R_{LM}, I_{tot} and U_{max}:

$$R_\Delta \leq \frac{u_{max} R_{LM}}{R_{LM} I_{tot} - u_{max}} \tag{2}$$

I_{tot} is divided between two branches formed by R_Δ and R_{LM}. This flowing current is reduced during the resistance profile motion. The exact value of the switch

current (i.e. I_{tot}) is calculated in each small time steps and inequality 2 is established based on the exact value of the total current as a function of time. Accordingly, the small increments of R_{Δ} per unit length of LM tail are obtained.

IV.2. Arcless Current Commutation

A. Steady State Arcs

Separation of two current carrying contacts results in initiation of switching arcs, if the voltage difference of the separating contacts exceeds a minimum level u_{min}^{arc} dependent on the contact material [13]. That is:

$$\Delta u < u_{min}^{arc} \tag{3}$$

Considering the equivalent circuit of Fig. 2, the arcless commutation constraint can be expressed as:

$$I_{tot}\left(R_{\Delta} - \frac{R_{\Delta}R_{LM}}{R_{\Delta} - R_{LM}}\right) < u_{min}^{arc} \tag{4}$$

Therefore the maximum allowable resistance profile gradient for given values of R_{LM}, I_{tot} and u_{min}^{arc} is calculated as:

$$R_{\Delta} < \frac{u_{min}^{arc}}{2I_{tot}}\left(1 - \sqrt{1 - \frac{4R_{LM}I_{tot}}{u_{min}^{arc}}}\right) \tag{5}$$

To check the switch performance in the transient recovery voltages (TRV), equivalent circuit shown in Fig. 3 should be analyzed. In normal condition all switches of Fig. 3 are closed except the load bypass switch, K_1. The current mainly flows through the nominal contact, K_2 (i.e., the conductive contact in Fig. 1). As the resistance profile is fully immersed in the LM, the resistive contact may carry a very small portion of the switch current depending on the resistance of nominal current contacts. The abnormal condition starts when the load bypass switch, K_1, is closed. The current suddenly increases and the moving contact starts to move in upward direction and the nominal current contact is separated (that means the switch K_2 is opened). Then, the current flows through the resistive contact and the contact resistance rapidly increases. Accordingly, the circuit current is reduced to a small amount which is proper for arcless switching. Due to the varying resistance profile, the circuit should be analyzed based on the linear time varying circuit concept. Since the temperature coefficient of resistance is small enough for the prescribed composition (5×10^{-5} K/°C from 20 to 1000 °C), the assumption of linearity of resistance profile is not far from reality.

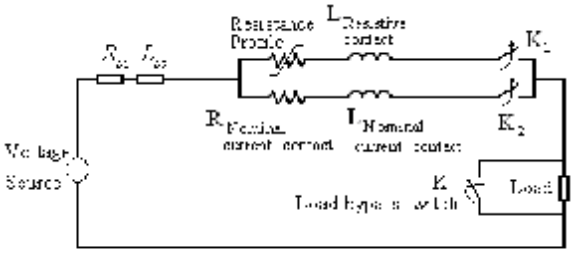

Fig. 3. Equivalent circuit of the system for TRV calculation

Essentially the waveform of the TRV is closely depended on the system parameters but it should be considered that due to the resistance profile of the contact, the X/R ratio of the circuit would be small before the contact separation. The resistance profile is designed in such a way that the circuit current just before contacts separation is below the minimum current needed for steady arc discharge. Therefore, having no thermo-field emission, insulation of the interruption medium should just be designed considering TRV waveform. The equivalent circuit of Fig. 3 can be described by equation (6):

$$u_{Source} = L_{sc}\frac{di(t)}{dt} + (R_{sc} - R_{tot})i(t) - u_{contacts} \tag{6}$$

The resulted contacts voltage should not exceed a minimum level u_{min}^{arc}:

$$u_{contacts} < u_{min}^{arc} \tag{7}$$

In other words, the voltage drop across the short contact gap should be less than minimum breakdown voltage of the insulating material. This voltage is also closely depended on the contact geometry. In the present study, the geometry and insulation material are not optimized from insulation point of view. Therefore, the selected test voltage is less than the minimum breakdown strength of air according to Paschen's law [14].

B. Arc Modes of short Length and Duration and Thermal Considerations

There are also a number of further arc modes which appear in extremely short gaps which are not stable [15]. These arc modes require minimum current and voltage values much lower than those of the steady arc discharge. Low current break arcs may pass some of these transient modes and they may lead to the steady arc. Bridge transfer is known as a way to prevent the apparent arc and facilitate "arcless switching" [15]. Once the resistance profile is separating from the LM, the LM bridge diameter decreases continuously while the constriction resistance and consequently the contact voltage/temperature in the contact constriction area

increase. The LM bridge prevents contact separation due to the surface tension. As the temperature inside the LM bridge increases, both viscosity and surface tension of the LM decrease. The bridge forms a catenoid. Before breakup, some small droplets may be separated from the LM bridge. Then it becomes weak and breaks at a contact distance of about 0.1mm. In the conventional switch contacts, directly after contact separation, evaporation of contact material is the main source of charged particles. Cathodes made from nonrefractory materials with a low boiling point, such as copper and mercury, experience significant material evaporation. These materials emit electrons at temperatures too low for thermionic emission and the emission of electrons is due to electric field emission [16]. In the proposed structure, the metal transfer in the switching contacts is not significantly affected by temperature (unlike to what happens in the molten metal bridge in normal solid contacts). However, the temperature of the LM bridge in the proposed structure indirectly influences the contingent arc phenomena following contact separation. Hence, the LM bridge temperature is of great importance. The temperature rise of the LM bridge can be overestimated. The heat loss energy in the LM bridge can be expressed as:

$$Q_{Bridge\ heat\ loss} = \int_0^{T_0} R_{LM}(t)\, I_{LM}^2(t)\, dt \qquad (8)$$

The time interval T_0 is selected from the moment which resistance profile is pulled out from the LM bulk and the LM bridge is formed till the breakup moment of the bridge which is depended on the motion velocity. To overestimate the LM bridge temperature rise, it is assumed that maximum switching current flows through the LM bridge when the formed catenoid has the minimum possible inner diameter considering the LM properties. In [17] the relationship between radius and length of dark contact bridge (in contrast with luminous bridge) is well elaborated. A similar approach is used to estimate the length and diameter of the bridge born from the specific a-spot which survived as a last one among multiple a-spots. The geometry is modeled in the FEM solver and the maximum LM bridge resistance just before breakup ($R_{LM_{max}}$) is calculated. Accordingly the maximum heat loss energy is calculated. Then, assuming adiabatic condition, the final temperature of the LM bridge is estimated with the following equation [18]:

$$T_f - \frac{Q_{Bridge\ heat\ loss}}{m_{LM\ tail} C_{LM}} \quad T_i \qquad (9)$$

T_i is in fact the temperature of the LM just before LM bridge formation which should be adopted considering the fact that before LM bridge formation and break up, the LM and its surrounding coolant medium (i.e. insulating fluid) have been heated up due to the heat losses in the resistance profile. Neglecting the heat losses in the metallic vessel, the total heat dissipated in the interruption chamber can be expressed as:

$$Q_{Resistive\ heat\ loss} = \int_0^{T} R_{Resistance\ Profile}(t)\, i^2(t)\, dt \qquad (10)$$

T is the total current commutation time interval. It starts from the moment that current is transferred to the resistance profile and ends when the current reaches zero. The left side integral of equation 10 is easily calculated considering the resistance profile increments and motion velocity. Assuming interruption chamber as an adiabatic system, the temperature change in the two phase mixture of LM and insulating fluid (IF) can be expressed as:

$$Q_{Resistive\ heat\ loss} = m_{LM} C_{LM} \Delta T + m_{IF} C_{IF} \Delta T \qquad (11)$$

where ΔT is the maximum temperature rise of the interruption chamber during resistance profile motion and before LM bridge formation (e.g., with respect to ambient temperature). It should be noted that in the present study, it is not intended to optimize the resistance profile and LM vessel dimension. In the experimental results, it will be explained that there is a considerable margin in the thermal design of the switch. However, more precise thermal analysis may be needed to optimize the switch dimension.

V. Drive Mechanism

If an externally triggered operation is intended, the proposed contact system can be developed to an arcless switch by any fast and powerful drive mechanism which fulfills the minimum required speed (in our case it is about 2m/s). As the moving contact is heated up during current interruption, the speed of drive mechanism plays a critical role in the switch operation. For a system with current limiter, the limiting action should be taken before actuation of other protective devices. In the present study, the current limiting action is a subsidiary goal which is needed in the proposed structure for arcless switching. For inherently triggered operation, the critical aspect is to pull out the resistance profile and transfer the current to the resistive path by means of built in energy of the system during abnormal condition. The resistance profile is implemented in an aerodynamic geometry to reduce the opponent shear force. To demonstrate the proposed principle, high speed electromagnetic repulsion and permanent magnet spring (PMS) structure [9] are used for switch operation. But the method has to be modified in respect of the driving force and speed due to the different requirements. In inherently operated switch, the repulsion coils are fed by the switch current and are

designed in such a way that once the current exceeds its threshold value, the resistance profile starts to move upward. Accordingly the normal contacts are separated and the current is transferred to the current limiting /interrupting system including the LM vessel and the resistance profile. Hence, while the resistance profile is in upward motion, the current flowing in the repulsion coils and the driving force are decreased. Meanwhile, the opponent force is also decreased as the resistance profile is pulled out from the LM bulk. In comparison with PMS used for the vacuum circuit breakers [9], less retaining force is needed for close status of the switch as the LM contact resistance is small enough needless to considerable pressure load on the contacts. Actually, the contact weight is adequate force to keep contacts closed despite the electromagnetic repulsion that occurs between the contacts at relatively high current. In contrast, due to the decreasing current and driving force, the PMS should provide more force during contacts separation. This is provided through a fixed U shaped permanent magnet and a cubic armature at the end of moving contact. Based on the specified threshold current, the resistance profile geometry, moving contact weight and motion profile the repulsion coils are designed in such a way that the resulted repulsion force prevails over the opponent forces and would throw the moving contact into the affected area of PMS. The repulsion force between two coaxial coils can be expressed as [19]:

$$F_{12} = a_z I_1 I_2 \frac{3\mu_0 N_1 N_2 \pi b_1^2 b_2^2 d}{2\left(d^2 - b_2^2\right)^{5/2}} \qquad (12)$$

Equation (12) is only used as a preliminary estimation. Once the main structure is designed, the motion time interval is broken to small time steps and in each step the geometry is modeled in the FEM solver. The model includes the coils of the electromagnetic repulsion mechanism and neglects eddy currents in the conductive parts. It calculates the force based on the current obtained from the analysis of the circuit in corresponding time step (i.e., depended on the position of the resistance profile). In each step, the force calculated in the electromagnetic transient FEM solver is assumed as an external body force for the moving contact. The calculated force is used in the simplified form of motion equation.

The procedure is similar to the method used in [20] for motion analysis but as the resistance profile is partly immersed in the LM and partly in the insulating fluid, the friction coefficient introduced in [20] and [8] may have an error in the velocity dependent opponent force [8] which essentially has a minor effect in the speed and the force profile. The possible error can easily be compensated by adjusting N_1.

VI. Experimental Study

To demonstrate the proposed principle for arcless switching, a switch is designed and made according to the described method. The prototype is designed to automatically interrupt 90A DC current without arc. From the preliminary experiments it was revealed that the LM tail in the geometry shown in Fig. 2 has a length of about 1.5mm when the moving contact speed lies between 1.6-2.3m/s. The contact resistance between copper part of the moving contact and the LM bulk in steady condition was not measurable. While the copper part of the moving contact is being pulled out from the LM bulk the measured resistance is of about 11 mΩ. This resistance is calculated through loss calculation where the losses of the various parts were not separable. The resistance profile is designed based on the constraints described in (2) to (7). Based on the results of [8], the LM tail resistance is about 6 mΩ. The maximum voltage u_{max} over the LM tail, at which no thermal overstress occurs, is in the range of 2 to 3V and u_{min}^{arc} for the LM contact is of about 13V. Among these ranges, the most stringent assumptions are taken to design the resistance profile. The total resistance of the moving contact is 10.3 Ω at room temperature which fulfills the gradient imposed by equations (2) and (5). One important aspect in the design of resistance profile is the length of the profile which should not be larger than some centimeters due to the limitations of drive speed. This resistance is implemented in 5 centimeter length spiral structure and is pulled out by an average speed of 2m/s. Care should be taken regarding the permitted surface loading (W/cm^2) of the resistive materials and their possible chemical reactions. The contact materials have been tested from wetability point of view. The contact angle of 1mm diameter LM droplets on the resistor material is greater than 150 degree. Possible chemical reactions, especially in high temperatures, have also been studied. It was observed that no chemical reaction occurs between the LM and resistance profile when the average temperature of the interruption chamber is 175 °C. The resistance profile carries current only in abnormal condition when the switch current exceeds the predetermined threshold value. The nominal switch DC current is 21.5 A. The test circuit used in the experiments is same as Fig. 3. A 15 V DC voltage source (i.e., greater than u_{min}^{arc}) and its parallel capacitor bank provide currents with amplitudes up to about 100A peak. The total circuit series inductance is of about 1mH to 5mH, which results in current waveforms with different rise-times. Fig. 4 shows the switch current and voltage for a short circuit test performed by closure of load bypass switch across the load in Fig. 3. As it can be seen at t = 12 ms the load is bypassed by switch K_1 and the current suddenly jumps from 12A to 89A. Due to low circuit resistance, the parallel capacitor bank of the voltage source starts to discharge much faster. At t = 25 ms, while the switch current is of about 30A, the conductive contact is

completely separated from the LM bulk (K_2 is opened), at this time a step-like increase of the resistance occurs, it must be noted that the voltage step has to be kept under u_{max}. The current commutates to the resistance profile and continuously decreases. This current commutation results in a considerable current reduction and switch voltage increase. Figure 5 shows the quantities of Fig. 4 with smaller Time/Div. In this figure, it is illustrated that at $t = 32\text{ms}$, the current reaches below the amount allowable for arcless current interruption. At this moment the resistance profile separates from the LM bulk and the last formed LM bridge is broken (K_3 is opened).

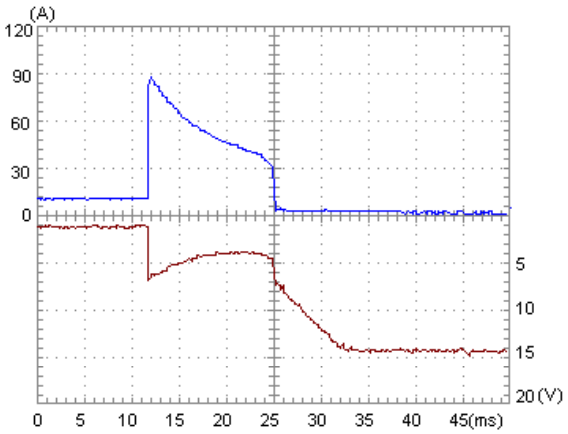

Fig. 4. Switch current and voltage during transition of normal load current to abnormal short circuit current and arcless interruption

At the beginning of resistance profile motion, the LM tail has a sudden change in the length as it is separating from the copper part and transferring to the surface of the resistance profile. Since the LM wets the surface of the copper part, the LM tail is drawn a little longer and when the LM separates from the copper part, the resistance increment which had been bridged over by the long LM tail comes into the circuit and caused the sudden voltage drop marked in Fig. 5.

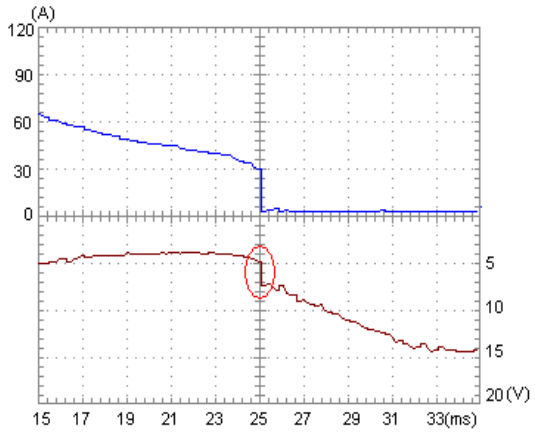

Fig. 5. Time zoom in the recorded switch current and voltage

It must be noted that this experiment is done just to investigate the proposed principle. Therefore to make it applicable in a real power circuits, the interaction of other system equipment and circuit parameters on the current waveform and resistance profile should be considered.

VII. Thermal Conditions and Hot Spot Motion

Equation (11) is used to overestimate the temperature rise of the contacts, it is assumed that the dissipated resistive heat loss is only expended to heat up the LM mass (m_{LM}). This would result in a temperature rise greater than real situation. It is revealed that even with the most pessimistic assumptions, i.e. the minimum drive speed and LM mass, the temperature rise of the interruption chamber would not be more than 23 °C. Furthermore, the specific heat of the LM, C_{LM}, is estimated through the method given in [21]. With most stringent assumptions for equation (9), the temperature rise of the LM bridge within the acceptable range of switch currents would not exceed 17.5 °C. It is notable that the contribution of the thermal conduction would result in even less temperature rises. Therefore, if the initial temperature of the interruption chamber is less than some 160 °C the LM bridge temperature would not reach the boiling point of the LM at atmospheric pressure. Hence, no metal vapor would be presented after contact separation. Therefore thermal-field emission of electrons would not be initiated.

To have an exact estimation of $R_{LM}$and its dissipated heat power, the current density distribution in the last LM bridge formed between LM bulk and resistance profile is simulated in the FEM solver (i.e., the most difficult condition for thermal overstressing). Considering the method described in [17], the worst possible LM bridge geometry is determined and the excitations are extracted from circuit analysis. The LM tail geometry is meshed with elements with length smaller than 0.03mm. The analysis is performed with 20 passes and the error is limited to 1%. Figure 6 shows current density distribution at the endmost moment of current interruption.

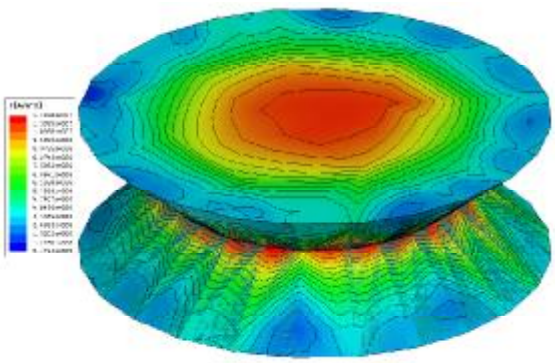

Fig. 6. Current density distributions in the LM bridge during current interruption

The resistance is calculated considering the total heat loss power evaluated in the concerned part and the excitations currents given as input to the solver. In the sample switch the total heat loss power calculated for the last LM bridge is less than 2.6 mW for 1A of the flowing current.

Due to the magnetic field of repulsion coils which is perpendicular to the current density vectors in the LM, a tangential circular force is exerted on the LM bulk surrounding the immersed contact. Figure 7 shows the force directions obtained from the interaction of the magnetic field and current density vectors in the FEM solver in magnetostatic simulation.

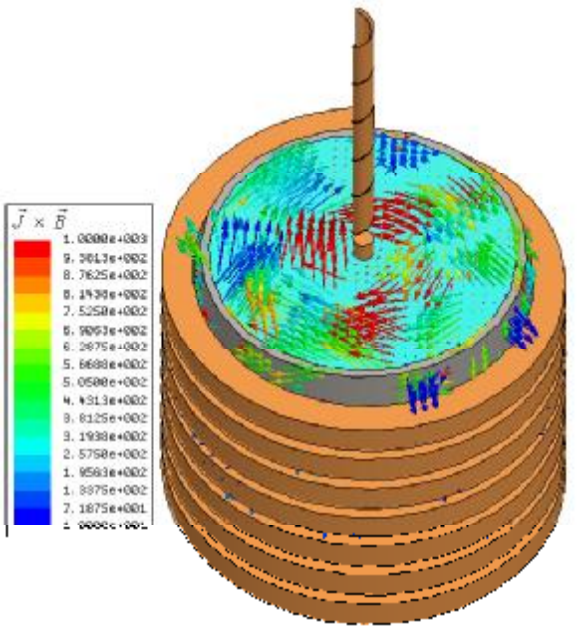

Fig. 7. Tangential Lorentz force exerted on the LM

The matter is also investigated through a simple experiment. A small marker particle is positioned on the LM level and the contact is fixed in its position inside the LM bulk. Nominal DC current flows through the fixed repulsion coil, conductive vessel, LM, and the moving repulsion coil. Figure 8 shows 3 picture frames taken from the LM level and the marker in time steps of 642 seconds. As it can be seen the marker moves in a spiral like path. The radial motion is due to the temperature gradient formed around the hot body (i.e., the immersed contact) and the subsequent fluid dynamics.

Fig. 8. Picture frames of the marker motion on the LM level due to the tangential Lorentz force

This spiral motion of LM around the immersed contact causes hot spots motion and reduces the LM temperature rise around the hot resistive contact during normal operation of the switch. It is notable that as it was intended to operate the switch at relatively high current, the turn number of the fixed repulsion coil has been reduced to prevent unwanted actuation at low nominal currents. The tangential force could be stronger if more magneto motive force would be provided.

A. *Stability in Transient Conditions*

The designed structure is modeled in the FEM solver in 2ms time steps. In each position the force is calculated and used in the motion equation [20] to obtain the next position. From the stability point of view the steady state position of the moving contact including the resistance profile and moving repulsion coil is of utmost importance as any transient current would cause a force which may lead to a small vertical motion of the immersed part.

In the sample switch the immersed contact has 8mm free conductive part between the resistance profile (which is located under the LM level) and the moving repulsion coil (which is located above the LM level). This free conductive area stabilizes the switch in the system transients. To evaluate the switch behavior in the system transient, the ratio of the Lorentz force to the quadratic of current amplitude is calculated in first 3 time steps of the motion. The average of the mentioned ratios is used as a proportionality coefficient (K_{Device}) between the Lorentz force ($F_{Lorentz}$) and square of the current:

$$F_{Lorentz} = K_{Device} I^2 \tag{13}$$

This formula along with the motion equation is used to obtain the moving contact vibration amplitude versus the normalized transient current amplitude. Maximum vertical displacement of the immersed contact with respect to the equilibrium position is shown in Fig. 9. Time duration of the current transient is used as a parameter.

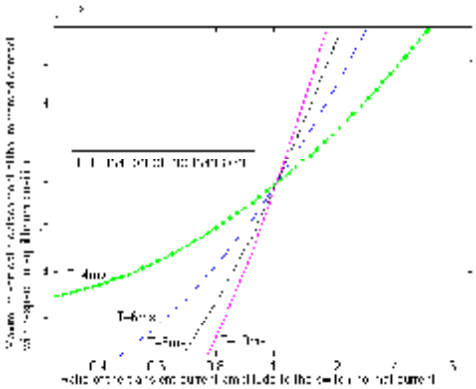

Fig. 9. Maximum vertical displacement of the immersed contact versus normalized transient current

The effect of buoyancy force of the LM on the immersed contact has not been taken into account in this stability analysis. It should be noted that vibration amplitude larger than 8mm (free conductive length) would cause a current limiting effect since such amount of vertical motion would bring a portion of the resistance profile above the LM level. Study of these types of vibrations should take the effect of the system interaction and parameters into account.

VIII. Replacement of the Anode and Cathode

As the experiments performed with DC current, in a quite similar test the assignment of the LM vessel (the fixed contact) and the resistance profile (moving contact) to the cathode was replaced and no significant difference was observed in the results. Since the current amplitude was the main concern of arcless switching in this study, this is not far from the expectation as there was no arc and its subsequent free ions in the interruption medium. But the matter should be studied when higher voltage level is required.

IX. Conclusion

This paper presents a method for controlled arcless current interruption. The working principle of the proposed switch is based on the motion of a resistance profile inside the liquid metal medium under the influence of Lorentz force. The phenomena relating to the arcless current interruption have been investigated and the relevant theoretical constraints have been derived and the thermal considerations of the contact separation have been studied. A high speed inherently operated drive system has been designed for the switch and the driving force was simply regulated through correction of coils turn numbers. Then a switch has been made to study the proposed method. The experimental results indicate that no arc occurs during current interruptions. The switch takes the advantage of the controllable arcless operation without external triggering. Moreover due to the liquid metal intermediate medium between the contacts, some usual problems of conventional switches like surface degradation of contacts can be avoided. At the end some features of the switch like stability in the transients and hot spot motion have been discussed. As the drive mechanism of the sample prototype is not fast enough, the switch did not show a perfect independent current limiting characteristic for practical application. Due to the motion of heated resistance profile in the LM vessel, there is always the risk of LM vaporization though in our experiments it was not detectable. For higher voltage applications, a profound study should be performed to optimize the contact and LM vessel geometry to prevent insulation breakdown after separation.

Acknowledgments

This work was supported by Iran National Science Foundation through Grant No. 86064/26.

References

[1] L. Chaabane, M. Sassi, A.S. Bouazzi, "Structural change of low voltage electrical switches under the effect of electrical arc erosion," *International Review of Electrical Engineering*, Vol. 2, No. 1, pp. 1-4, Jan.-Feb. 2007.

[2] H. Schmitt et al., "Fault Current Limiters – State of the Art," CIGRE Working Group 13.10, 2002.

[3] M. Lindmayer, "High temperature superconductors as current limiters – an alternative to contacts and arcs in circuit breakers," in Proc. 39th Int. Conf. on Electrical Contacts, pp. 1 – 10, 1993.

[4] W. Paul et al., "Fault current based on high temperature superconductors – different concepts, test results, simulations, applications," PHYSICA C 354, pp. 27-33, 2001.

[5] R. Strumpler et al., "Novel medium voltage fault current limiters based on polymer PTC resistors," IEEE Trans. on Power Delivery, Vol. 14, No. 2, pp. 430-435, Apr. 1999.

[6] W. W. Chen "A Method to Achieve Arcless Interruptions in Low Current Power Circuits," IEEE Trans. Components and Packaging Technologies, Vol. 24, No. 3, pp. 363-369, Sept. 2001.

[7] A. Krätzschmar, F. Berger, P. Terhoeven and S. Rolle, "Liquid metal current limiters," in Proc. 20th Int. Conf. Electrical Contacts, pp. 167 – 172, 2000.

[8] K. Niayesh, J. Tepper and K. Koenig, "A Novel Current Limitation Principle Based on Application of Liquid Metals," IEEE Trans. Components and Packaging Technologies, Vol. 29, No. 2, pp. 303-309, June 2006.

[9] M. Tsukima et al., "Development of a High-Speed Electromagnetic Repulsion Mechanism for High-Voltage Vacuum Circuit Breakers," Electrical Engineering in Japan, Vol. 163, No. 1, pp. 34-40, 2008.

[10] M. Braunovic, V. Konchits and N. K. Myshkin, Electrical Contacts; Fundamentals, Applications and Technology, New York: Taylor & Francis Group, LLC, 2006.

[11] A. Fairweather, "The closure and partial separation of a metallic contact," in Proc. IEE Part II, vol. 92, pp. 301-321, 1945.

[12] P. Slade, Electrical Contacts: Principals and Applications, New York, Marcel Decker Inc., 1999.

[13] R. Holm, Electric Contacts: Theory and applications, Springer Verlag, Berlin, Germany, 4th edition, 2000.

[14] E. Kuffel, W.S. Zaengle and J. Kuffel, High Voltage Engineering Fundamentals, Butterworth-Heinemann, Great Britain, 2000.

[15] W. F. Rieder, "Low Current Arc Modes of Short Length and Time: A Review," IEEE Trans. on Components and Packaging Technologies, Vol. 23, No. 2, pp. 286-292, June 2000.

[16] L. van der Sluis, Transients in Power Systems, England, John Wiley & Sons Ltd, 2001.

[17] H. Ishida et al., "Relationship between length and diameter of contact bridge formed under thermal equilibrium condition," IEICE Trans. Electron, Vol. E88-C, No. 8, Aug. 2005.

[18] J. H. Leinhard, A Heat Transfer Textbook, 3rd ed., Cambridge Massachusetts, USA, Phlogiston Press, 2006.

[19] D. K. Cheng, Field and wave Electromagnetic, 2nd ed., MA, Addison-Wesley, 1983.

[20] P. Pourmohamadiyan and K. Niayesh, "Conceptual design of a novel arcless controlled switch," Springer, Electrical Engineering, Vol. 90, No. 8, pp. 529 538, 2009.

[21] H. Cord, "A Literature Survey on Fluid Flow Data for Mercury-Constitutive Equation," European Spallation Source (ESS), paper 81-T; December 1998.

[22] Adam, M.; Baraboi, A.; Pancu, C.; Plesca, A., Aspects Regarding the Controlled Switching of the Circuit Breakers, *International Review of Electrical Engineering (IREE)*, Vol. 3, n. 5, 2008, pp. 759-767.

Authors' information

School of Electrical and Computer Engineering
University of Tehran
Tehran, Iran
School of Electrical and Computer Engineering, Faculty of Engineering, University of Tehran,
Po Box: 14395-515, IR-14395-Tehran
E-mails: pmohmad@ut.ac.ir
kniayesh@ut.ac.ir
mohseni@ut.ac.ir

Pedjman Pourmohamadiyan was born in Tehran, Iran, on September 21, 1976. He received the B.Sc. degree in Electrical Engineering from Shiraz University, Shiraz, Iran, in 1998. He received his M.Sc. and PhD degree in Electrical Engineering from University of Tehran, Tehran, Iran, in 2001 and 2010 respectively. Since 1999, he has been working with various industries as a test inspector of HV&MV apparatuses, senior electrical engineer and electrical lead engineer. Through these experiences he has collected data of various test results and failures which have been used in academic researches.

Kaveh Niayesh (S'98 M'01-SM'09) was born in Tehran, Iran, on July 19, 1971. He received the B.Sc. and M.Sc. degrees from Tehran University, Tehran, Iran, in 1993 and 1996, respectively, and the Ph.D. degree from the Aachen University of Technology, Aachen, Germany, in 2001, all in electrical engineering. He has been with the High Voltage Systems Group, ABB Corporate Research, Baden-Daettwil, Switzerland, from 2001 to 2005, before joining the School of Electrical and Computer Engineering, University of Tehran in 2005 where he is currently teaching as an associate professor.

Hossein Mohseni was born in Tehran, Iran, in 1942. He studied electrical engineering at Technical University Graz, Austria, and received the Dipl.-Ing. and Dr.-techn. degrees in 1971 and 1975, respectively. From 1971 to 1976 he was with ELIN Union AG Austria, working as testing and research engineer in the high voltage laboratory and the Transformer R&D department. In 1976 he joined the Faculty of engineering, University of Tehran. He is currently a professor of electrical engineering, head of High voltage laboratory of University of Tehran and teaches high voltage, insulation technology and transient in power system and apparatus. He is also a technical consultant with the Iran Power Generation and Transmission Company (TAVANIR).